

# Physics-Informed Neural Networks for Discovering Localised Eigenstates in Disordered Media

Liam Harcombe<sup>a</sup>, Quanling Deng<sup>a,\*</sup>

<sup>a</sup>*School of Computing, Australian National University, Canberra, ACT 2601, Australia*

---

## Abstract

The Schrödinger equation with random potentials is a fundamental model for understanding the behaviour of particles in disordered systems. Disordered media are characterised by complex potentials that lead to the localisation of wavefunctions, also called Anderson localisation. These wavefunctions may have similar scales of eigenenergies which poses difficulty in their discovery. It has been a longstanding challenge due to the high computational cost and complexity of solving the Schrödinger equation. Recently, machine-learning tools have been adopted to tackle these challenges. In this paper, based upon recent advances in machine learning, we present a novel approach for discovering localised eigenstates in disordered media using physics-informed neural networks (PINNs). We focus on the spectral approximation of Hamiltonians in one dimension with potentials that are randomly generated according to the Bernoulli, normal, and uniform distributions. We introduce a novel feature to the loss function that exploits known physical phenomena occurring in these regions to scan across the domain and successfully discover these eigenstates, regardless of the similarity of their eigenenergies. We present various examples to demonstrate the performance of the proposed approach and compare it with isogeometric analysis.

**Keywords:** Schrödinger equation, Hamiltonian, Anderson localisation, eigenvalues and eigenstates, neural networks, isogeometric analysis

---

## 1. Introduction and Background

Partial differential equations (PDEs) are powerful tools for studying dynamic systems and have applications across various fields. However, these equations are notoriously difficult to solve explicitly, leading to an increased interest in numerical approximations. In addition to classical numerical methods, recent

---

\*Corresponding author

Email addresses: u7100338@anu.edu.au (Liam Harcombe), Quanling.Deng@anu.edu.au (Quanling Deng)

research has shown the potential of using neural networks to estimate solutions to differential equations.

There are several advantages of using neural networks to solve PDEs over traditional numerical methods. Firstly, neural networks are generally efficient as they can often produce solutions to PDEs more quickly than traditional numerical methods, particularly for high-dimensional problems. Secondly, they are more robust against the “curse of dimensionality,” which refers to the difficulty of solving PDEs in high-dimensional spaces using traditional numerical methods. Furthermore, they can be trained to solve a wide range of PDEs, including those with complex boundary conditions or nonlinear operators. Once trained, neural networks can quickly produce solutions for new PDEs that are similar to those encountered during training, potentially without requiring further adjustments or recalibration of parameters. Overall, neural networks can provide a powerful and flexible tool for solving PDEs, especially in cases where traditional numerical methods may be insufficient or computationally expensive.

Data-driven supervised networks [10] and data-free unsupervised networks [13] have been shown to produce efficient approximations of differential eigenvalue problems. Supervised networks aim to discover patterns in labelled datasets to infer a general model that can predict examples outside of the given dataset. The training process involves calculating approximations for given inputs and computing how much these estimations deviate from the true outputs using a loss function. Then, the networks minimise this loss function by adjusting their parameters. Artificial Neural Networks (ANNs) are comprised of layers of interconnected nodes with weights and biases that calculate the estimations. Convolutional Neural Networks (CNNs) are a newer form of neural networks that are especially known for their ability to identify patterns faster and more reliably than ANNs in solving eigenvalue problems using labelled datasets [10]. They introduce a convolutional layer built up of windows that slide around the input data, searching for patterns in whole regions at a time. They are commonly used to pass the information on to ANNs and are optimised similarly. In situations where training data do not contain labels, unsupervised networks are proposed to tackle the given task. These networks rely on a carefully designed loss function based on known information about the desired result to push the network toward a correct approximation.

In the case of finding the eigenstates of Hamiltonians, we leverage known physical phenomena to design our loss function. This kind of model is an example of a Physics Informed Neural Network (PINN, c.f., [2, 20]), one that embeds the knowledge of physical laws governing the system into the learning process to drive the network to an admissible approximation.

Differential eigenvalue problems occur in a wide range of problems in physics and applied mathematics, such as quantum energy problems. In early works, Lagaris et al. [15] proposed an ANN to discover the solu-

tions to differential eigenvalue problems, tested on various problems in quantum mechanics. More recently, Finol et al. [10] presented a supervised ANN to solve eigenvalue problems in mechanics, showing that CNNs were outperforming traditional ANNs in contexts with labelled datasets. Sirignano and Spiliopoulos [21] developed a deep learning network to accurately solve partial differential equations in dimensions as high as 200. They also proposed a mesh-free algorithm, which was desirable as meshes become infeasible in such high dimensions. Chen et al. [3] adopted the emerging PINNs to solve representative inverse scattering problems in photonic metamaterials and nano-optic technologies. Their method was also mesh-free and was tested against numerical simulations based on the finite element method. These ANN models are excellent at learning time series data. The work [18] demonstrated its application in wave packet displacements in localised and delocalised quantum states. Another work [14] adopted CNNs to solve a classification problem. The authors constructed a supervised model learning from experimental data to distinguish between the dynamics of an Anderson insulator and a many-body localised phase. Yang et al. [23] proposed a combination of PINNs with Bayesian Neural Networks, which solved both forward and inverse nonlinear problems, obtaining more accurate predictions than PINNs in systems with large noises.

Jin et al. [13] have shown that PINNs can solve single and multiple square well problems, calculating the eigenfunction and eigenvalue simultaneously. Their network employs a scanning mechanism that pushes the network to search for higher eigenstates as the training process evolves, while the network updates the eigenfunction prediction accordingly. They store found eigenfunctions and exploit the orthogonality of wave functions to search for higher eigenstates. Grubišić et al. [11] applied PINNs to identify localised eigenstates of operators with random potential. They studied the effective potential of the operator, whose local minima correspond to the different eigenstates. They first built a PINN to solve these eigenvalue problems in one dimension, then generalised to a deeper model that solves higher dimensional problems. Effective potentials provide a neat way of locating the localised eigenstates, however, are limited in the number of locations they can identify, and have difficulty differentiating between eigenstates of identical eigenvalue. These limitations occur in Bernoulli distributed potentials, which we aim to solve with our model.

We build on the design of [13] to approximate these eigenstates for Hamiltonians whose potentials are distributed randomly, leading to the localisation of the solution to specific regions of the domain. In particular, the core of our work is in finding these eigenstates where the eigenenergies are nearly identical, a task that current models are unable to accomplish. This is most prevalent with potentials distributed according to the Bernoulli distribution but can occur in other distributions.

The rest of the paper is organised as follows. In Section 2, we state the Schrödinger differential eigen-

value problem and present the isogeometric analysis, followed by a discussion on the challenges of its spectral approximation. In section 3, we propose our novel loss function design for the PINN for solving the Schrödinger equation. Section 4 collects and discusses various numerical tests to demonstrate the performance of the proposed method. Concluding remarks are presented in section 5.

## 2. Problem Statement and Isogeometric Analysis

In this section, we first introduce the modelling problem, followed by a presentation of a classic numerical method, namely isogeometric analysis, used to solve the problem as well as to generate the reference solutions. We then provide a general discussion on the challenges associated with the numerical computation of the model.

### 2.1. Problem Statement

We study the time-independent Schrödinger equation: Find the eigenpair  $(E, u)$  such that

$$\begin{aligned} \left[ -\frac{\hbar^2}{2m}\Delta + V \right] u &= Eu \quad \text{in } \Omega, \\ u &= 0 \quad \text{on } \partial\Omega, \end{aligned} \tag{2.1}$$

where  $\Delta = \nabla^2$  is the Laplacian,  $V = V(x) \in L^2(\Omega)$  specifies the potential and is a non-negative function, and  $\Omega \subset \mathbb{R}^d$ ,  $d = 1, 2, 3$ , is a bounded open domain with Lipschitz boundary  $\partial\Omega$ . Throughout the paper, we will focus on the case with  $d = 1$ , followed by a discussion on its extension to  $d = 2, 3$ . The differential operator is referred to as the Hamiltonian, i.e.,  $\mathcal{H} = -\frac{\hbar^2}{2m}\Delta + V$ . Here,  $\hbar$  is the reduced Planck constant and  $m$  is the mass of the particle. Without loss of generality, this equation is equivalent to:

$$\begin{aligned} -\Delta u + Vu &= Eu \quad \text{in } \Omega, \\ u &= 0 \quad \text{on } \partial\Omega. \end{aligned} \tag{2.2}$$

This problem is a Sturm-Liouville eigenvalue problem (see, for example, [9, 22]) which has a countable infinite set of positive eigenvalues  $E_j \in \mathbb{R}^+$

$$0 < E_1 < E_2 \leq \dots \leq E_j \leq \dots \tag{2.3}$$

with an associated set of orthonormal eigenfunctions  $u_j$

$$(u_j, u_k) = \int_{\Omega} u_j(x) u_k(x) \, d\mathbf{x} = \delta_{jk}, \tag{2.4}$$

where  $\delta_{jk}$  is the Kronecker delta which is equal to 1 when  $j = k$  and 0 otherwise. The set of all the eigenvalues is the spectrum of the Hamiltonian. We normalise the eigenfunctions in the  $L^2$  space; hence, the

eigenfunctions are orthonormal under the scalar inner product. Let us define two bilinear forms

$$a(w, v) = \int_{\Omega} \nabla w \cdot \nabla v + V w v \, d\mathbf{x} \quad \text{and} \quad b(w, v) = (w, v) = \int_{\Omega} w v \, d\mathbf{x}, \quad \forall w, v \in H_0^1(\Omega), \quad (2.5)$$

where  $H_0^1(\Omega)$  is the Sobolev space with functions vanishing at the boundary  $\partial\Omega$ . Using this notation, the eigenfunctions are also orthogonal with each other with respect to the energy's inner product, i.e.,

$$a(u_j, u_k) = (-\Delta u_j + V u_j, u_k) = (E_j u_j, u_k) = E_j (u_j, u_k) = E_j \delta_{jk}, \quad (2.6)$$

where we have used the integration by parts on (2.2). We remark that these orthogonalities are critical in the development of the proposed neural networks in Section 3.

## 2.2. Isogeometric Analysis

Let  $H_0^1(\Omega)$  be the standard Hilbert space where both functions and their weak derivatives are in  $L^2(\Omega)$  with functions vanishing at the boundary. At the continuous level, the weak formulation for the eigenvalue problem (2.2) is: Find all eigenvalues  $E \in \mathbb{R}^+$  and eigenfunctions  $u \in H_0^1(\Omega)$  such that,

$$a(w, u) = E b(w, u), \quad \forall w \in H_0^1(\Omega), \quad (2.7)$$

while at the discrete level, the isogeometric analysis (IGA, c.f., [4, 6, 8, 12]) for the eigenvalue problem (2.2) is: Find all eigenvalues  $E_h \in \mathbb{R}^+$  and eigenfunctions  $u_h \in W_h$  such that,

$$a(w_h, u_h) = E_h b(w_h, u_h), \quad \forall w_h \in W_h(\Omega), \quad (2.8)$$

where  $W_h \subset H_0^1(\Omega)$  is the solution and test space spanned by the B-spline or non-uniform rational basis spline (NURBS) basis functions [5].

In this paper, for comparison with the state-of-the-art, we adopt the recently-developed soft isogeometric analysis (softIGA, c.f., [7, 16]). SoftIGA has a similar variational formulation as (2.8) which leads to the matrix eigenvalue problem

$$\mathbf{K}\mathbf{U} = E_h \mathbf{M}\mathbf{U}, \quad (2.9)$$

where  $\mathbf{K}_{ab} = a(\phi_a, \phi_b)$ ,  $\mathbf{M}_{ab} = b(\phi_a, \phi_b)$ , and  $\mathbf{U}$  contains the coefficients of the eigenfunction  $u_h$ , for its representation in the linear combination of the B-spline basis functions. For simplicity, the matrix  $\mathbf{K}$  (although it contains a scaled mass) is referred to as the stiffness matrix while the matrix  $\mathbf{M}$  is referred to as the mass matrix, and  $(E_h, \mathbf{u}_h)$  is the unknown eigenpair. We refer to [7, 16] for details.

### 2.3. A Few Challenges on Numerical Computation

There are a few challenges in the numerical computation, such as using IGA or softIGA, of the Schrödinger equation with random potentials. Firstly, there is a non-uniqueness of solutions. The Schrödinger equation with random potentials can have multiple solutions that correspond to the same (or very similar) energy level. This non-uniqueness can make it difficult to accurately identify the correct eigenstates, particularly when dealing with complex potential landscapes. Secondly, it can be a multi-scale problem with large sampling/discretisation errors. Random potentials can vary over multiple length scales, which leads to inaccurate numerical simulations and can make it challenging to choose an appropriate discretisation size and mesh. Thirdly, the Schrödinger equation for many-body problems in multiple dimensions suffers from the curse of dimensionality. The number of parameters needed to describe the random potential can be very large. As the number of dimensions increases, the computational cost of solving the Schrödinger equation can increase exponentially.

Last but not least, the Schrödinger equation with random potentials is a complex mathematical problem, and solving it numerically can be computationally expensive. This is particularly true for large system sizes and high disorder strengths, which require a large number of numerical simulations. Moreover, solving the Schrödinger equation with a different random potential requires constructing a new matrix eigenvalue problem (2.9), which can be a time-consuming process. This can become particularly challenging when solving the equation for a large number of random potentials. In such cases, one potential solution is to train a neural network that takes the random potential as input and produces the corresponding eigenstates as outputs. For instance, to solve the Schrödinger equation with  $N$  different random potentials, one could use a classic method like softIGA and apply it  $N$  times, or alternatively, train a neural network using data from a subset of cases ( $N_0 \ll N$ ) and then use the well-trained neural network to solve the remaining cases. This approach can save a significant amount of computational time, particularly when  $N$  is large. With these challenges in mind, we introduce the following neural-network-based method as an alternative method to solve the Schrödinger equations.

### 3. The Physics-Informed Neural Networks

Deep neural networks are a type of machine learning algorithm inspired by the structure and function of the human brain. They are composed of multiple layers of artificial neurons, each performing a nonlinear transformation of the input data. The output of each layer is fed as input to the next layer, allowing the network to learn increasingly complex features and relationships in the data.

Some common types of deep neural networks include convolutional neural networks (CNNs) for image processing and computer vision tasks, recurrent neural networks (RNNs) for sequential data processing, deep belief networks (DBNs) for unsupervised learning, and generative adversarial networks (GANs) for image and video synthesis. Deep neural networks have demonstrated impressive performance in many applications. In this paper, we adopt the physics-informed neural networks (PINN) with a novel loss function design to solve the Schrödinger equations.

### 3.1. PINN

The PINNs are simply feed-forward neural networks (FNNs) where the loss functions are defined based on the physics laws (typically PDEs) [17, 20]. The PINNs algorithm combines the flexibility and efficiency of neural networks with the accuracy and interpretability of PDEs, making it a powerful tool for solving complex PDEs in a wide range of scientific and engineering applications. The major steps of the PINNs for solving a PDE are as follows:

1. Construct a neural network: The first step is to define the architecture of the neural network that will be used to approximate the solution to the PDE. This typically involves specifying the number and activation functions of layers in the network, as well as the number of neurons in each layer.
2. Define the loss function: The loss function is used to measure the error between the predictions of the neural network and the actual solution to the PDE. In PINNs, the loss function typically includes terms that enforce the PDE and any associated initial or boundary conditions.
3. Train the neural network: The neural network is trained by minimizing the loss function using an optimisation algorithm, such as stochastic gradient descent (SGD).
4. Validate the solution: Once the neural network has been trained, it can be used to make predictions about the solution to the PDE. The accuracy of the predictions can be assessed using validation data that have not been used during training.
5. Refine the solution: If the accuracy of the predictions is not satisfactory, the neural network can be further refined by adjusting the network architecture, loss function, or optimisation algorithm, and then retraining the network.

Typically, the loss function in PINN is defined as

$$L = L_{\text{de}} + L_{\text{reg}}, \quad (3.10)$$

where  $L_{\text{de}}$  specifies the loss associated with the PDE and  $L_{\text{reg}}$  specifies the loss associated with the regularisation such as the boundary conditions. The loss function term  $L_{\text{de}}$  involves derivatives which are usually

evaluated by the automatic differentiation by Tensorflow [1] or by Pytorch [19]. In the following subsection, we present a goal-oriented loss function for the best performance in solving the Schrödinger equations with random potentials.

### 3.2. Loss Function Design

To demonstrate the main idea, we focus on the one-dimensional case. We assume that the potential  $V(x)$  is randomly distributed over  $m$  regions over the domain  $[0, 1]$ , and each region has a random value. Each set of random values then characterises the individual differential eigenvalue problem to be solved for Anderson localised states. We partition the interval  $[0, 1]$  into  $n + 1$  equally spaced points  $x_j = jh, j = 0, 1, \dots, n$  where  $h = 1/n$  is the grid/mesh size. We denote by  $\mathbf{u}_h = (u_h(x_0), u_h(x_1), \dots, u_h(x_n))^T$  as a vector of the approximate values of the true solution  $u(x)$  at each of these coordinates  $x_j$ . Similarly, we denote by  $\mathbf{V} = (V(x_0), V(x_1), \dots, V(x_n))^T$  as a vector of the approximate values of the potential  $V(x)$ . In our PINN model, we use choose  $n$  such that each region has exactly 5 nodes each for accuracy as well as for training efficiency. To approximate the second derivative vector  $u''(x)$ , we use the centre finite difference method with an accuracy order of six, i.e., the error is of  $\mathcal{O}(h^6)$ .

We construct a PINN that takes the vector  $\mathbf{V}$  as input and split it into two separate networks: one that calculates the eigenvalue ( $E$ ), and the other one for the eigenfunction  $u(x)$ . Figure 3.1 draws this model structure, highlighting the split into separate networks. We set the number of nodes in each hidden layer to  $n$ , allowing the network to scale with the size of the mesh.

The driving force of this network towards a correct solution is the design of its loss function, which is built of multiple terms relating to different aspects of a correct solution. The neural network's optimisation method (backpropagation) works to minimise the loss function, so we choose terms that are positive errors for incorrect predictions of  $E$  and  $u(x)$  and are zero for correct predictions. Thus, the minimisation of these terms leads the network to produce correct predictions for  $E$  and  $u(x)$ .

The central term of our loss function is the term:

$$L_{\text{de}} = \sqrt{\frac{1}{n+1} \sum_{i=0}^n (E_h u_h(x_i) + u_h''(x_j) - V(x_j) u_h(x_j))^2} \quad (3.11)$$

which is always non-negative and is zero for solutions  $E$  and  $u(x)$  that satisfy equation 2.2; thus, it satisfies the consistency condition. To encourage the network to satisfy the boundary conditions  $u(0) = u(1) = 0$ , we create the term:

$$L_{\text{bound}} = u_h^2(x_0) + u_h^2(x_n) \quad (3.12)$$



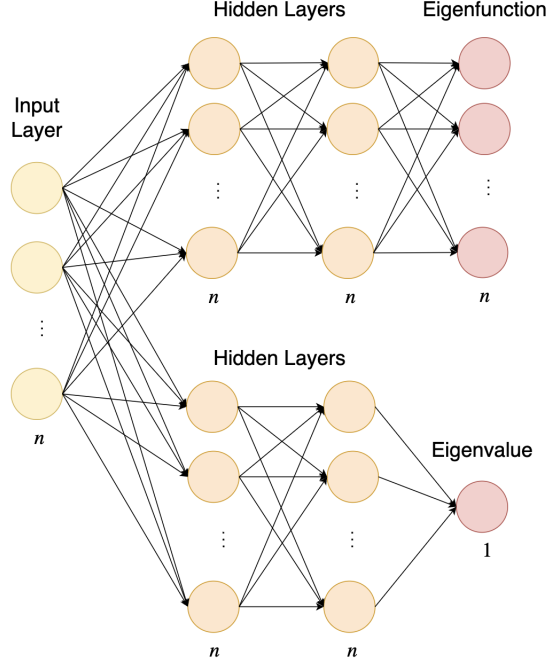


Figure 3.1: Neural network structure for the prediction of eigenstates of Hamiltonians.

which the minimisation of the loss function leads to  $u_h(x_0) = u_h(x_n) = 0$ . The major issue with using just these terms is that the trivial solution  $u(x) = 0$  satisfies these terms (reducing them to zero). Thus, we need the following term to penalise the approximate solution:

$$L_{\text{norm}} = \left( \int_0^1 u_h(x) dx - 1 \right)^2. \quad (3.13)$$

The minimisation of this loss term leads to approximate solutions of  $L^2$  norm 1. For the integration, we use the mid-point rule and this calculation is majorly local. In the PINN model developed in [13], this condition was imposed using the terms like  $1/u^2(x)$  and  $1/E^2$ . We point out that since the eigenstates are localised, an eigenstate  $u(x) = 0$  for most of the domain, leads to very large and even infinite values due to the design of the term  $1/u^2(x)$ . Consequently, this leads to difficulties in minimising the loss function and the overall neural network training. Our design of the loss term 3.13 is novel, sufficient, and computationally efficient to approximate normalised non-trivial solutions.

These terms are sufficient to push the network to generate an admissible eigenstate. However, the model often produces the same eigenstates, preventing the discovery of higher states. To overcome this issue, once

an eigenstate  $(E_h, u_h(x))$  is discovered, we add the eigenstate  $u_h(x)$  to a list of eigenstates  $S$ . Then, we take advantage of the known physical fact that the eigenfunctions of Hamiltonians are orthogonal and construct the following term:

$$L_{\text{orth}} = \sum_{\hat{u}_h(x) \in S} \left( \int_0^1 \hat{u}_h(x) u_h(x) dx \right)^2, \quad (3.14)$$

where  $u_h(x)$  is the network's current state to be produced. We iteratively recompile and train the network, collecting the eigenstates once the prediction is acceptable. To decide whether a prediction is admissible, we determine whether  $L_{\text{de}}$  is below a certain threshold, as well as a patience condition as in [13] that checks if the absolute value of the change in  $L_{\text{de}}$  and that of the eigenvalue is below another threshold. This allows the network to converge to solutions with  $L_{\text{de}}$  much lower than the chosen threshold, given that it is converging fast enough.

In this study, we discover that these terms are sufficient in training the model to discover multiple eigenstates, without the use of the drive term described in [13]. The loss function we have built so far performs adequately on problems with enough spread in the eigenvalues between different states. However, in situations where the eigenstates have nearly identical eigenvalues, the network in [13] is unable to distinguish between the states, converging to an undesirable algebraic combination of the eigenfunctions. We believe this is due to that the local minima in the high dimensional loss function graph that represent the correct eigenstates are much closer when the eigenvalues are similar, causing difficulty in the optimisation process. When studying Hamiltonians with potentials generated randomly, there is a disorder for Anderson localisation to occur. We leverage this fact in our loss function with the following procedure.

We let the model run with the above loss function for a certain number of epochs  $q$ , which is a hyperparameter. The goal is to set this parameter so that at epoch  $q$ , the network has converged to an algebraical combination of the eigenfunctions; for example, see the left plot in Figure 3.2.

Since we know the eigenstates of the Hamiltonian are localised, each spike in 3.2 represents a separate localised state. We thus scan through the eigenfunction and generate a list  $K$  of the regions of the domain where the norm of the eigenfunction is greater than some set hyperparameter, splitting apart the regions where the function returns to zero to separate the localised spikes. Then, in our iterative process of discovering eigenvalues, at each step we choose one of the intervals in  $K$  (say,  $[x_a, x_b]$ ) and add the following term to the loss function:

$$L_{\text{loc}} = \left( \int_0^1 u_h(x) d\mathbf{x} - \int_{x_a}^{x_b} u_h(x) d\mathbf{x} \right) \quad (3.15)$$

which encourages the network to set the eigenfunction to zero outside of the localisation interval  $[x_a, x_b]$ .

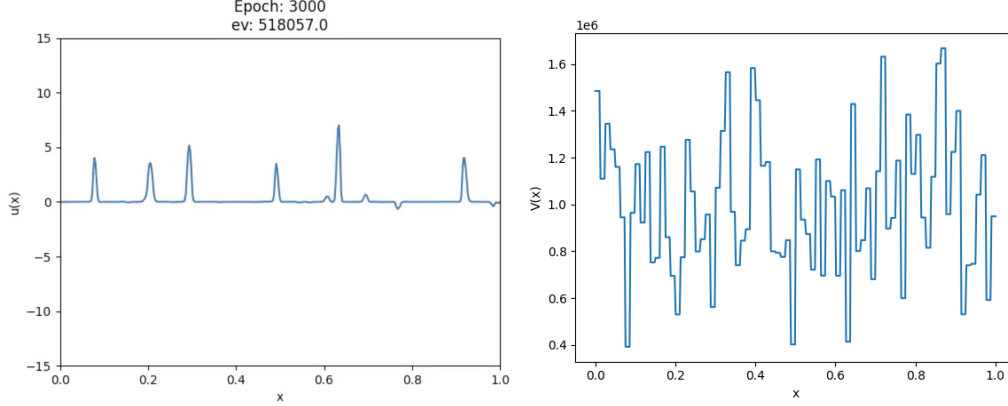


Figure 3.2: Left: An example of an algebraic combination of eigenstates where their eigenenergies are approximately equal. Right: The corresponding potential  $V(x)$  with  $m = 80$  uniform elements, where  $V(x)$  is randomly generated in each element according to the normal distribution with mean 1 and standard deviation 0.3, scaled by  $10^6$ .

Equivalently, we could have added terms like  $L_{\text{end}}$  for each nodal point outside of  $[x_a, x_b]$ . We remark that this term is non-negative. With all these loss terms in mind, then we have

$$L_{\text{reg}} = L_{\text{bound}} + L_{\text{norm}} + L_{\text{ort}} + L_{\text{loc}}, \quad (3.16)$$

which is added to  $L_{\text{de}}$  to give the overall loss function  $L$  in (3.10). Throughout the paper, we use this novel loss function in our proposed PINN with the structure shown in Figure 3.1.

#### 4. Numerical Experiments

We test our PINN model on various Hamiltonians with randomly distributed potential and demonstrate the network's robustness against potential with different distributions. In particular, we consider potentials with distributions that cause the Hamiltonian to admit eigenstates with almost identical eigenenergies. This is most prevalent in potentials distributed according to the Binomial distribution. We test the network against various values for  $m$  with and choose  $n$  such that there are five nodes for each of the  $m$  regions of the potential.

The localised states usually occur in the region where the potential takes its smallest value. When there are multiple disjoint regions at (or very close to) this minimum value, each of these regions can admit a localised state, where they all can have similar eigenenergy. Figure 4.3 shows the first four PINN approximated eigenstates where the potential is shown in the right plot of Figure 3.2. The network can distinguish between the first three eigenstates, regardless of how similar their eigenvalues are. We observe that if  $u(x)$

satisfies equation 2.2, then  $-u(x)$  also satisfies it.  $-u(x)$  also has the same  $L^2$  norm as  $u(x)$ , so it satisfies all other terms in our designed loss function. However, the network is demonstrated to be robust in such cases. For consistency, we plot all eigenfunctions in their positive form.

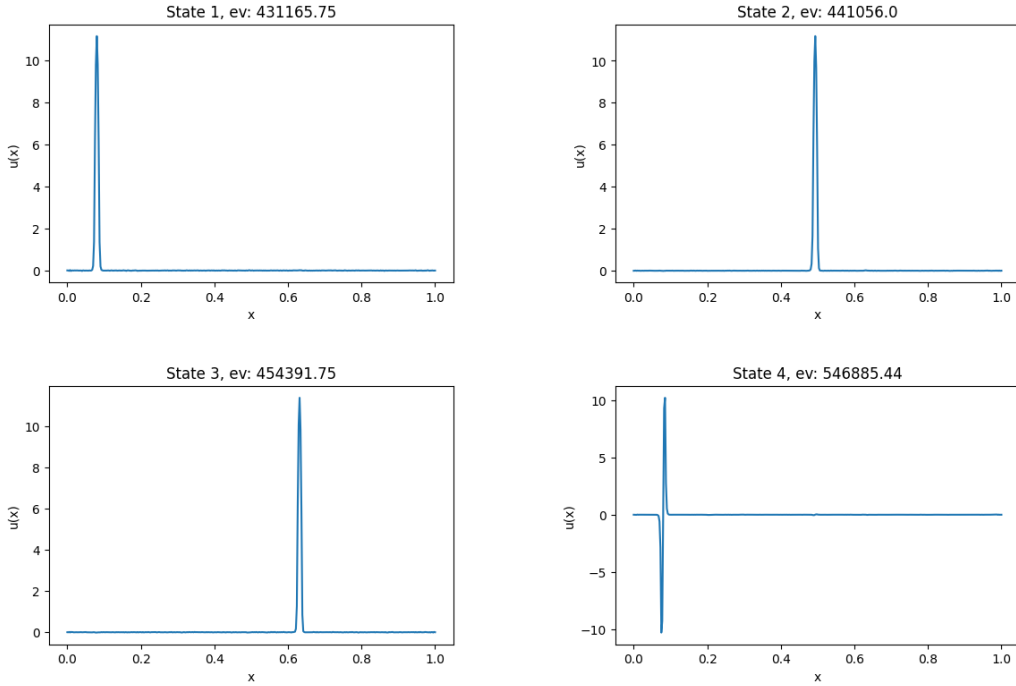


Figure 4.3: The first four PINN approximated eigenstates with the potential defined in the right plot of Figure 3.2.

Figure 4.4 shows a potential with a Bernoulli distribution, while Figure 4.5 shows the first four eigenstates, the first three of which have almost identical eigenvalues. We expect these eigenstates to localise in the “troughs” of the potential, which is what we observe in the eigenfunction plots. The states that localise in troughs of similar length tend to have almost the same eigenvalue, which our model captures.

Figure 4.6 shows the model’s prediction of the eigenvalue as the training process evolves. After 2000 epochs, the model adds the  $L_{\text{loc}}$  term. The model produces converging eigenvalues until around epoch 9000. At this point, the model’s prediction has met the convergence criteria and saves the eigenstate to use in  $L_{\text{orth}}$  and it resets its weights to search for the next eigenstate. In our implementation, we include a function that generates a video to display the network’s eigenfunction prediction as the training process evolves, which is

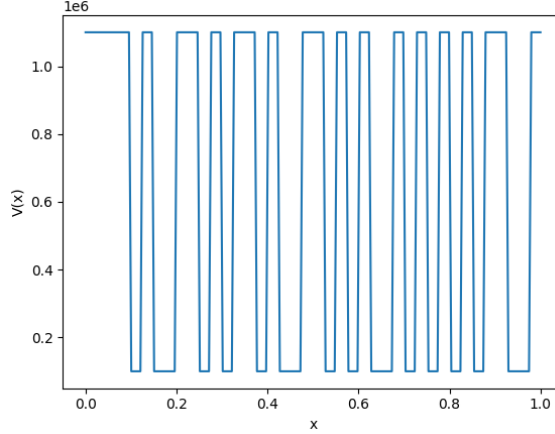


Figure 4.4: The potential  $V(x)$  with  $m = 40$  uniform elements, where  $V(x)$  was randomly generated in each element according to the Bernoulli distribution with probability 0.5, scaled by  $10^6$  and shifted up by  $10^5$ .

available at our GitHub<sup>1</sup> page.

Table 1 displays the PINN eigenvalue errors where we use the reference eigenvalues generated by the softIGA method with a very fine mesh ( $C^1$  quadratic splines with 2000 elements). We also test the model's robustness against the number of nodes. We note that the model achieves slightly better results for the potential distribution according to the normal distribution compared to the uniform distribution. This may be due to that the points generated by the normal distribution are more concentrated around the mean than in the other cases. However, the results for the Bernoulli distributed potentials are much better, all with relative errors below 1%. This demonstrates the success of our approach to the problem of eigenstates with similar eigenvalue. Table 2 displays the eigenvalue prediction results for a single potential generated by the Bernoulli distribution with a different number of mesh elements. As the number of elements increases, there is a clear improvement in the accuracy of the PINN-predicted eigenvalues. The convergence rate is of order approximately 2 but the theoretical analysis of this convergence is subject to future study.

## 5. Concluding Remarks

Recently, there has been a growing interest in using machine learning and neural networks to solve differential equations, particularly in the study of Hamiltonians. In this paper, we extend current models by constructing a neural network that is capable of distinguishing eigenstates from Hamiltonians with randomly

---

<sup>1</sup><https://github.com/liamharcombe4/eigen-network>

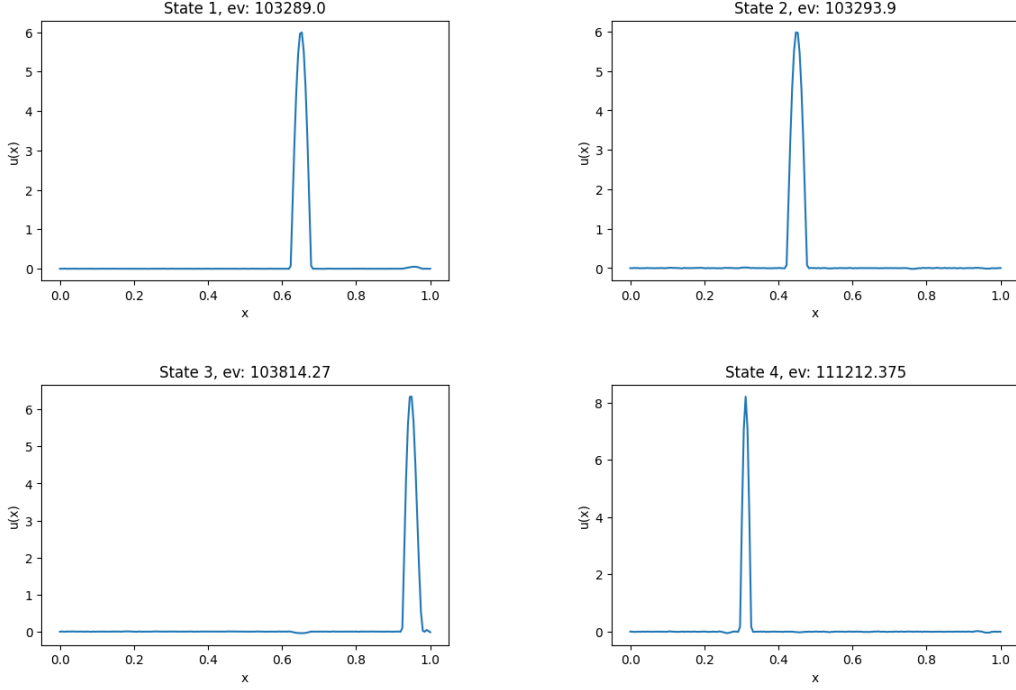


Figure 4.5: The first four PINN approximated eigenstates with the potential defined in Figure 4.4.

Potential Distribution	Nodes ( $n + 1$ )	Regions ( $m$ )	Eigenvalue Error (%)
Normal	400	80	0.863
Normal	200	40	1.16
Normal	100	20	0.123
Bernoulli	200	40	0.351
Uniform	200	40	1.92

Table 1: The relative eigenvalue errors of the PINN-approximated first eigenenergy of Hamiltonians with potentials generated according to various distributions.

distributed potentials that lead to localisation in the states. Our approach involves incorporating a normalisation loss term to avoid trivial solutions and an orthogonal loss term to search for higher eigenstates. Our method eliminates the need for driving terms, which can hinder a network’s ability to converge to an admissible solution. The novelty of our approach lies in a new localisation loss term, which encourages the network to converge to a solution that is localised to a specific region. This idea is based on the physical

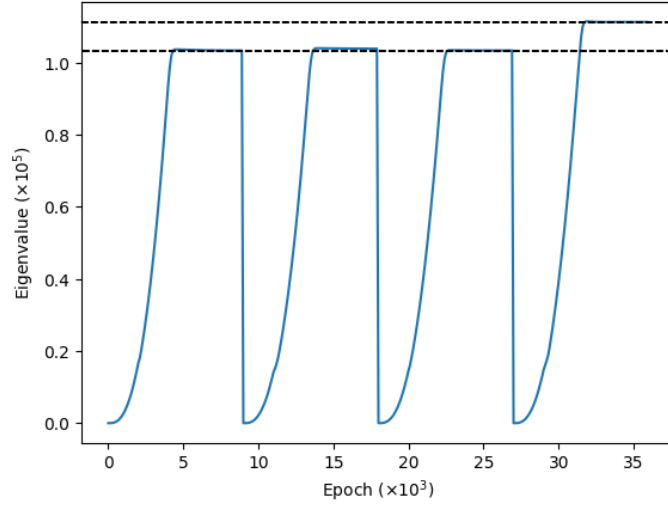


Figure 4.6: The eigenvalue prediction with respect to the epoch (training process) using the potential in Figure 4.4. The dotted lines represent the true eigenvalues.

Nodes ( $n + 1$ )	Eigenvalue Error (%)
100	0.783
200	0.343
300	0.0512

Table 2: The relative eigenvalue errors of the PINN-approximated first eigenenergy of Hamiltonian with a fixed Bernoulli distributed potential over  $m = 20$  regions.

fact that localised eigenstates occur in randomly distributed potentials. We utilise the network’s initial attempt at convergence to identify regions of localised states before adding this term to achieve the desired approximation. We demonstrate the effectiveness of our approach in discovering eigenstates for potentials generated randomly according to different distributions, with the highlight being the Bernoulli distribution, which leads to eigenstates with identical eigenvalue. Our model successfully predicts these eigenstates with good accuracy, overcoming a challenge faced by current models.

There are several potential avenues for future work. Some potential future directions in this research area include: (1) exploring the use of more complex loss functions that can capture additional physical constraints, such as symmetries or conservation laws; (2) investigating the use of different network architectures, such as convolutional neural networks or attention-based models, to improve accuracy and scalability; (3)

generalising the approach to higher-dimensional systems or non-linear differential equations; and (4) investigating the performance of the approach with larger and more complex systems, including systems with a larger number of particles or more complex interactions. Overall, the use of ANNs to solve differential equations and approximate eigenstates of Hamiltonians has shown to be a promising approach, and there are many potential directions for future research in this area.

## References

- [1] M. Abadi, P. Barham, J. Chen, Z. Chen, A. Davis, J. Dean, M. Devin, S. Ghemawat, G. Irving, M. Isard, et al. Tensorflow: a system for large-scale machine learning. In *OsdI*, volume 16, pages 265–283. Savannah, GA, USA, 2016.
- [2] S. Cai, Z. Mao, Z. Wang, M. Yin, and G. E. Karniadakis. Physics-informed neural networks (PINNs) for fluid mechanics: A review. *Acta Mechanica Sinica*, 37(12):1727–1738, 2021.
- [3] Y. Chen, L. Lu, G. E. Karniadakis, and L. D. Negro. Physics-informed neural networks for inverse problems in nano-optics and metamaterials. *Opt. Express*, 28(8):11618–11633, Apr 2020.
- [4] J. A. Cottrell, T. J. Hughes, and Y. Bazilevs. *Isogeometric analysis: toward integration of CAD and FEA*. John Wiley & Sons, 2009.
- [5] C. de Boor. *A practical guide to splines*, volume 27 of *Applied Mathematical Sciences*. Springer-Verlag, New York, revised edition, 2001.
- [6] Q. Deng. Isogeometric analysis of bound states of a quantum three-body problem in 1D. In *Computational Science – ICCS*, pages 333–346, Cham, 2022. Springer International Publishing.
- [7] Q. Deng, P. Behnoudfar, and V. M. Calo. SoftIGA: Soft isogeometric analysis. *Computer Methods in Applied Mechanics and Engineering*, 403:115705, 2023.
- [8] Q. Deng, V. Puzyrev, and V. Calo. Isogeometric spectral approximation for elliptic differential operators. *Journal of Computational Science*, 2018.
- [9] L. C. Evans. *Partial differential equations*, volume 19 of *Graduate Studies in Mathematics*. American Mathematical Society, Providence, RI, second edition, 2010.
- [10] D. Finol, Y. Lu, V. Mahadevan, and A. Srivastava. Deep convolutional neural networks for eigenvalue problems in mechanics. *International Journal for Numerical Methods in Engineering*, 118, 01 2018.



- [11] L. Grubišić, M. Hajba, and D. Lacmanović. Deep neural network model for approximating eigenmodes localized by a confining potential. *Entropy*, 23(1), 2021.
- [12] T. J. R. Hughes, J. A. Cottrell, and Y. Bazilevs. Isogeometric analysis: CAD, finite elements, NURBS, exact geometry and mesh refinement. *Comput. Methods Appl. Mech. Engrg.*, 194(39-41):4135–4195, 2005.
- [13] H. Jin, M. Mattheakis, and P. Protopapas. Physics-informed neural networks for quantum eigenvalue problems. In *IJCNN at IEEE World Congress on Computational Intelligence*, 2022.
- [14] F. Kotthoff, F. Pollmann, and G. De Tomasi. Distinguishing an Anderson insulator from a many-body localized phase through space-time snapshots with neural networks. *Phys. Rev. B*, 104:224307, Dec 2021.
- [15] I. E. Lagaris, A. Likas, and D. I. Fotiadis. Artificial neural network methods in quantum mechanics. *Computer Physics Communications*, 104(1-3):1–14, 1997.
- [16] D. Li and Q. Deng. Soft isogeometric analysis of the bound states of a quantum three-body problem in 1D. *Journal of Computational Science*, page 102032, 2023.
- [17] L. Lu, X. Meng, Z. Mao, and G. E. Karniadakis. DeepXDE: A deep learning library for solving differential equations. *SIAM review*, 63(1):208–228, 2021.
- [18] T. Mano and T. Ohtsuki. Machine learning the dynamics of quantum kicked rotor. *Annals of Physics*, 435:168500, 2021. Special Issue on Localisation 2020.
- [19] A. Paszke, S. Gross, S. Chintala, G. Chanan, E. Yang, Z. DeVito, Z. Lin, A. Desmaison, L. Antiga, and A. Lerer. Automatic differentiation in pytorch. 2017.
- [20] M. Raissi, P. Perdikaris, and G. E. Karniadakis. Physics-informed neural networks: A deep learning framework for solving forward and inverse problems involving nonlinear partial differential equations. *Journal of Computational physics*, 378:686–707, 2019.
- [21] J. Sirignano and K. Spiliopoulos. Dgm: A deep learning algorithm for solving partial differential equations. *Journal of Computational Physics*, 375:1339–1364, 2018.
- [22] G. Strang and G. J. Fix. *An analysis of the finite element method*, volume 212. Prentice-Hall Englewood Cliffs, NJ, 1973.

- [23] L. Yang, X. Meng, and G. E. Karniadakis. B-pinns: Bayesian physics-informed neural networks for forward and inverse PDE problems with noisy data. *Journal of Computational Physics*, 425:109913, 2021.